

Review

Estimation of Hourly, Daily and Monthly Global Solar Radiation on Inclined Surfaces: Models Re-Visited

Seyed Abbas Mousavi Maleki ^{1,2,*}, H. Hizam ^{1,2} and Chandima Gomes ¹

¹ Department of Electrical and Electronic Engineering, Universiti Putra Malaysia, Serdang, 43400 Selangor, Malaysia; hhizam@upm.edu.my (H.H.); chandima.gomes@hotmail.com (C.G.)

² Centre of Advanced Power and Energy Research (CAPER), Universiti Putra Malaysia, 43400 Selangor, Malaysia

* Correspondence: abbas.maleki12260@yahoo.com; Tel.: +60-122-221-336

Academic Editor: Tatiana Morosuk

Received: 20 September 2016; Accepted: 23 December 2016; Published: 22 January 2017

Abstract: Global solar radiation is generally measured on a horizontal surface, whereas the maximum amount of incident solar radiation is measured on an inclined surface. Over the last decade, a number of models were proposed for predicting solar radiation on inclined surfaces. These models have various scopes; applicability to specific surfaces, the requirement for special measuring equipment, or limitations in scope. To find the most suitable model for a given location the hourly outputs predicted by available models are compared with the field measurements of the given location. The main objective of this study is to review on the estimation of the most accurate model or models for estimating solar radiation components for a selected location, by testing various models available in the literature. To increase the amount of incident solar radiation on photovoltaic (PV) panels, the PV panels are mounted on tilted surfaces. This article also provides an up-to-date status of different optimum tilt angles that have been determined in various countries.

Keywords: solar radiation model; tilt angle; isotropic and anisotropic; solar energy; hourly estimation

1. Introduction

At weather stations, the global solar radiation is generally measured on horizontal surfaces. Nevertheless, in order to take full advantage of the solar radiation on collector surfaces, conventional stationary solar systems, both solar photovoltaic and flat plate solar collectors, are mounted on inclined surfaces.

Hourly global solar radiation on inclined surfaces can be estimated from global solar radiation on horizontal surfaces using several models. The models can be used to estimate components of hourly global solar radiation on horizontal surfaces (for direct and diffuse radiation) and inclined surfaces (for direct, diffuse, and ground-reflected radiation). As the estimation models are strongly affected by the latitude of location, finding the most accurate model for each region is compulsory. The accurate model can be found by comparing the measured values and estimated values by different statistical indicators [1]. As the number of estimation models is many, generally researchers choose some models that have been found in previous studies as accurate models in different latitudes close to their region latitude. The lack of a review study based on recognizing the most accurate model in different locations is the motivation of this study.

Moreover, since the amount of solar radiation incident on a solar thermal collector or a photovoltaic panel is strongly affected by its installation angle and orientation [2–4], finding the optimum tilt angle to receive maximum solar radiation on a photovoltaic module is the cheapest and most effective method [5].

This paper is organized as follows:

Section 2 describes basic solar components. Section 3 provides the details and methods to estimate solar radiation components on horizontal surfaces and a summary of different studies that have been done to determine the most accurate models to estimate solar radiation on horizontal surfaces. The details and methods to estimate solar radiation components on inclined surfaces and a summary of different studies that have been done to determine the most accurate models to estimate solar radiation on inclined surfaces is given in Section 4. Section 5 describes the determination method of the optimum tilt angle and an update status of optimum tilt angles in various countries. The conclusion of the study is given in Section 6.

Although numerous models for estimation of diffuse radiation on horizontal and inclined surfaces have been developed in the last two decades, a study that classifies the adopted models by considering the affecting parameters such as latitude of different location and optimum tilt angle is notably lacking. This paper attempts to provide a comprehensive review of well-known proposed models for different geographic coordinates and to introduce the ones with the highest performance. The list of optimum tilt angles for different countries has also been updated. Such a review should help future investigations to choose the potential models suitable for their studied locations.

2. Basic Solar Components

• Declination Angle (δ)

Declination is the angular distance from the sun north or south to the earth's equator. As schematically illustrated in Figure 1, the maximum and minimum declination angle values of the earth's orbit produce seasons. Declination ranges between 23.45° north and 23.45° south. The northern hemisphere is inclined 23.45° far away from the sun some time around 21 December, which is the summer solstice for the southern hemisphere and the winter solstice for the northern hemisphere. In the northern hemisphere and through 21 June, starting around 21 June, the southern hemisphere is positioned in a way that it is 23.45° away from the sun; meanwhile, it is winter solstice in the northern hemisphere. During the fall and spring equinoxes, which begin on 21 March and 21 September respectively, the sun passes directly over the equator [6].

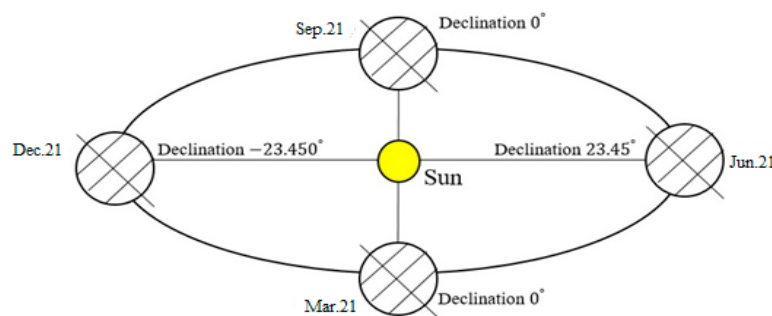


Figure 1. Maximum and minimum value of declination angle.

δ is the declination angle and it can be found from Spencer's [7] equation in radians.

$$\delta = (0.006918 - 0.399912 \cos \Gamma + 0.070257 \sin \Gamma - 0.006758 \cos 2\Gamma + 0.000907 \sin 2\Gamma - 0.002697 \cos 3\Gamma + 0.00148 \sin 3\Gamma) \left(\frac{180}{\pi} \right)$$

Here, Γ is the day angle in radians and is represented by

$$\Gamma = 2\pi \left(\frac{n-1}{365} \right)$$

where n is the number of the day in the year, for example 1 January = 1, 20 February = 51, and so on.

- **Hour Angle (ω)**

The concept of hour angle is used for describing the rotation of the earth around its polar axis which is equivalent to $+15^\circ$ per hour during the morning and -15° in the afternoon. It is the angular distance between the observer's meridian and the meridian whose plane contains the sun (Figure 2). The following equation can be used to calculate the hour angle in degrees. It should be noted that at noon the hour angle ω is zero [6].

$$\omega = 15(12 - ST)$$

where ST is the local solar time.

$$ST = LT + \frac{ET}{60} + \frac{4}{60}[L_s - L_L]$$

where LT is the local standard time, L_s is the standard meridian for a local zone, L_L is the longitude of the location under study in degrees and ET is the equation of time given by Tasdemiroglu [8] as:

$$ET = 9.87 \sin 2B - 7.53 \cos B - 1.5 \cos B$$

$$B = \frac{360(n - 81)}{365}$$

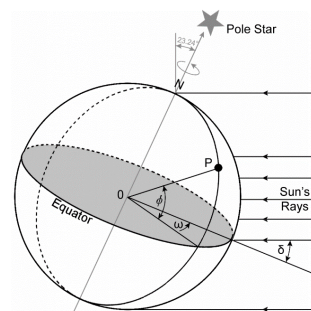


Figure 2. Hour angle (ω) for point P [9].

- **Solar Azimuth Angle (γ)**

The angular displacement from the south of the beam radiation projection on the horizontal plane is defined as the solar azimuth angle. This is schematically illustrated in Figure 3.

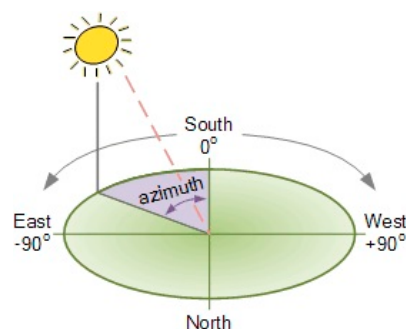


Figure 3. Definition of sun's azimuth angle.

- **Latitude (ϕ)**

The latitude of an area is the position with relevance north or south of the Equator. The variation of the latitude is from 0° to $\pm 90^\circ$ (positive for northern and negative for the southern hemisphere), 0° at the Equator and $\pm 90^\circ$ at the Poles.

- **Hourly Extraterrestrial Radiation (I_o)**

Extraterrestrial radiation is defined as the incidence of solar radiation outside the earth's atmosphere and is computed with the following equation:

$$I_o = \frac{12 \times 3.6}{\pi} I_{sc} E_0 \times \left((\sin \varphi \cos \delta) \times (\sin \omega_2 - \sin \omega_1) + \frac{\pi(\omega_2 - \omega_1)}{180} (\sin \varphi \sin \delta) \right)$$

where I_{sc} is a solar constant (1367 W/m^2); E_0 is the eccentricity correction factor [10]; δ is the declination angle; φ is the latitude of location; ω_1 and ω_2 are the hour angle at the beginning and end of the time interval, where all angles are given in degrees. The eccentricity correction factor E_0 can be calculated according to Spencer [7]. The following series gives the equation for time (in minutes).

$$E_0 = 1.000110 + 0.034221 \cos \Gamma + 0.001280 \sin \Gamma + 0.000719 \cos 2\Gamma + 0.000077 \sin 2\Gamma$$

For most engineering and technological applications, however, a very simple expression used by Beckman may be employed [10]:

$$E_0 = 1 + 0.0033 \cos \left(\frac{2\pi n}{365} \right)$$

3. Hourly Global Solar Radiation on Horizontal Surfaces (I_H)

Global solar radiation on horizontal surfaces can be measured with a pyranometer, which is an instrument that measures global solar radiation from all directions. The global solar radiation on horizontal surfaces can be categorized as follows:

- Diffuse solar radiation (I_b)
- Direct beam solar radiation (I_d)

Solar radiation on a horizontal surface is the sum of the horizontal direct and diffuse radiation.

$$I_H = I_d + I_b$$

3.1. Hourly Diffuse Radiation on Horizontal Surface (I_d)

Diffuse solar radiation is a part of the sunlight that passes through the atmosphere and is consumed, scattered or reflected by water vapor, dust particles or pollution. This type of radiation cannot throw sharp shadows and therefore cannot be focused [11].

Large numbers of meteorological/radiometric stations normally measure the received global irradiation on horizontal surfaces. It is not an easy task to collect such measurements, mainly due to the high price of the measuring equipment. For this reason, a number of mathematical models have been defined to estimate diffuse radiation on horizontal surfaces. The models that can determine diffuse radiation on horizontal surfaces can be classified into two types as follows:

- Parametric models
- Decomposition models

3.1.1. Parametric Models

Specific information of environmental conditions such as atmospheric turbidity, fractional sunshine, cloud cover, and perceptible water content are necessities of parametric models [12].

$$I_H = I_{bN} \cos \theta_z + I_d$$

$$I_{bN} = A \exp \left[\frac{-B}{\cos \theta_z} \right]$$

$$I_d = CI_N$$

where I_{bN} is normal solar beam radiation on horizontal surfaces, θ_z is the zenith angle and can be calculated from following equation:

$$\theta_z = \cos^{-1}(\sin \delta \sin \varphi + \cos \delta \cos \varphi \cos \omega)$$

A, B, C are values of constants and are given for each model in Table 1.

- **ASHRAE Model**

The ASHRAE algorithm offers a simpler method, which is widely utilized by the engineering and architectural communities [13,14].

- **Machler and Iqbal's Model**

Machler and Iqbal [15] studied estimating hourly diffuse irradiation from hourly global solar radiation measured on horizontal surfaces. They recommended investigating solar altitude ranges above 40°. They improved the invariables A, B and C (of the ASHRAE model), which considers the improvements in solar radiation research over the previous decades.

- **Parishwad's Model**

Parishwad et al. [16] assessed the constants of the ASHRAE model (A, B, and C) using statistical indicator analysis of measured solar radiation data of six cities from different locations in India.

- **Nijegorodov's Model**

Nijegorodov revised the constants of ASHRAE's model, using a computer program to predict hourly and daily global solar radiation in Botswana based on recorded solar radiation components in Botswana, Namibia, and Zimbabwe [17].

3.1.2. Decomposition Models

Decomposition models typically utilize only data pertaining to global radiation to estimate diffuse radiation from global solar radiation data. Decomposition models are based on a correlation between the diffuse and total radiation on a horizontal surface (M_t = clearness index). This correlation is defined as a function of the hourly clearness index (ratio of hourly global horizontal (I_H) to hourly extraterrestrial radiation (I_o)). The clearness index (M_t) is a measure of the atmospheric effects in an isolated place [18]. It is a random parameter that varies according to time of the year, season, climatic conditions, and geographical situation of a place [19].

$$M_t = \frac{I_H}{I_o}$$

- **Chandrasekaran and Kumar's Model**

In Madras, India, which is a tropical setting, Chandrasekaran and Kumar collected data using a fourth-order polynomial correlation [20]:

$$\text{For } 0 < M_t \leq 0.24 \quad I_d = (1.0086 - 0.178M_t)I_H$$

$$\text{For } 0.24 < M_t \leq 0.8$$

$$I_d = \left(0.9686 + 0.1325M_t + 1.4183M_t^2 - 10.1862M_t^3 + 8.3733M_t^4\right)I_H$$

$$\text{For } 0.8 < M_t \leq 1 \quad I_d = (1.0086 - 0.178M_t)I_H$$

Table 1. Estimated values of A, B, and C for different models.

	January	February	March	April	May	June	July	August	September	October	November	December
ASHARE												
A	1230	1215	1186	1136	1104	1088	1085	1107	1152	1193	1221	1234
B	0.142	0.144	0.156	0.180	0.196	0.205	0.207	0.201	0.177	0.160	0.149	0.142
C	0.058	0.060	0.071	0.097	0.121	0.134	0.136	0.122	0.092	0.073	0.063	0.057
Machler and Iqbal												
A	1202	1187	1164	1130	1106	1092	1093	1107	1136	1166	1190	1204
B	0.141	0.142	0.149	0.164	0.177	0.185	0.186	0.182	0.165	0.152	0.144	0.141
C	0.103	0.104	0.109	0.120	0.130	0.137	0.138	0.134	0.121	0.111	0.106	0.103
Parishwad et al.												
A	610.00	652.20	667.86	613.35	558.39	340.71	232.87	240.80	426.21	584.73	616.60	622.52
B	0.000	0.010	0.036	0.121	0.200	0.428	0.171	0.148	0.074	0.020	0.008	0.000
C	0.242	0.249	0.299	0.395	0.495	1.058	1.611	1.624	0.688	0.366	0.253	0.243
Nijgorodov												
A	1163	1151	1142	1146	1152	1157	1158	1152	1150	1156	1167	1169
B	0.177	0.174	0.170	0.165	0.162	0.160	0.159	0.164	0.167	0.172	0.174	0.177
C	0.114	0.112	0.110	0.105	0.101	0.098	0.100	0.103	0.107	0.111	0.113	0.115

- **Erbs' Model**

The same correlation types were used by Erbs and colleagues, applying data collected from five stations in the U.S. at different latitudes between 31° and 42°. The data range from 1–4 years, which is considered a short duration. Hourly values were registered at each of the stations for early normal direct radiation as well as global radiation on a horizontal surface. The difference between these quantities was calculated as diffuse radiation [21].

$$\text{For } 0 < M_t \leq 0.22 \quad I_d = (1 - 0.09M_t)I_H$$

$$\text{For } 0.22 < M_t \leq 0.8 \quad I_d = \left(0.9511 - 0.1604M_t + 4.388M_t^2 - 16.638M_t^3 + 12.336M_t^4\right)I_H$$

$$\text{For } 0.8 < M_t \leq 1 \quad I_d = 0.165I_H$$

- **Hawladar's Model**

Hawladar derived a second-order polynomial correlation from data gathered at a tropical site in Singapore [22].

$$\text{For } 0 < M_t \leq 0.225 \quad I_d = (0.915M_t)I_H$$

$$\text{For } 0.225 < M_t < 0.775 \quad I_d = \left(1.135 - 0.9422M_t - 0.3878M_t^2\right)I_H$$

$$\text{For } 0.775 \leq M_t \leq 1 \quad I_d = (0.215)I_H$$

- **Jacovides' Model**

Jacovides et al. considered the time interval between 1987 and 1992 in order to measure hourly pyranometric global and diffuse solar irradiation in Athalassa. The data were retrieved from the Cyprus Meteorological Service [23]. The correlations are presented as follows:

$$\text{For } 0 < M_t \leq 0.1 \quad I_d = (0.987)I_H$$

$$\text{For } 0.1 < M_t \leq 0.8 \quad I_d = \left(0.94 + 0.937M_t - 5.01M_t^2 + 3.32M_t^3\right)I_H$$

$$\text{For } 0.8 < M_t \leq 1 \quad I_d = (0.177)I_H$$

- **Karatasou's Model**

Karatasou et al. [24] suggested a third order polynomial correlation based on data gathered from Athens, Greece.

$$\text{For } 0 < M_t \leq 0.78 \quad I_d = \left(0.9995 - 0.05M_t - 2.4156M_t^2 + 1.4926M_t^3\right)I_H$$

$$\text{For } 0.78 < M_t \leq 1 \quad I_d = (0.2)I_H$$

- **Lam and Li's Model**

A similar effort was made by Lam and Li based on data measured for the time period between 1991 and 1994 in Hong Kong. They sought to find a correlation between global solar radiation and its components, whether direct or diffuse. Their hybrid correlation model was built upon hourly measured data in order to predict hourly direct and diffuse components from the global radiation for the given country [25]. The model is provided as follows:

$$\text{For } 0 < M_t \leq 0.15 \quad I_d = (0.977)I_H$$

$$\text{For } 0.15 < M_t \leq 0.17 \quad I_d = (1.237 - 1.361M_t)I_H$$

$$\text{For } 0.17 < M_t \leq 1 \quad I_d = (0.273)I_H$$

- **Louche's Model**

Louche et al. used the clearness index M_t to get an estimation on the direct radiation I_b with the following equation [26]:

$$\text{For } 0 < M_t \leq 1$$

$$I_b = \left(-10.676M_t^5 + 15.307M_t^4 - 5.205M_t^3 + 0.99M_t^2 - 0.059M_t + 0.02 \right) I_H$$

$$I_d = I_H - I_b$$

- **Miguel's Model**

Miguel and colleagues collected data from different Northern Mediterranean countries situated in the so-called Belt Area. They presented a third-order polynomial correlations for hourly diffuse radiation [27].

$$\text{For } 0 < M_t \leq 0.21 \quad I_d = (0.995 - 0.081M_t)I_H$$

$$\text{For } 0.21 < M_t \leq 0.76 \quad I_d = \left(0.724 + 2.738M_t - 8.32M_t^2 + 4.967M_t^3 \right) I_H$$

$$\text{For } 0.76 < M_t \leq 1 \quad I_d = (0.18)I_H$$

- **Orgill and Hollands' Model**

The correlation provided by Orgill and Hollands is the first of its kind which uses four years of data gathered in Toronto, Canada [28]. Sky cover is categorized into three classes in this correlation, as follows:

$$\text{For } 0 < M_t < 0.35 \quad I_d = (1 - 0.249M_t)I_H$$

$$\text{For } 0.35 \leq M_t \leq 0.75 \quad I_d = (1.577 - 1.84M_t)I_H$$

$$\text{For } 0.75 < M_t \leq 1 \quad I_d = (0.177)I_H$$

- **Boland's Model**

A mathematical approach called the Boland-Ridley-Lauret (BRL) model was employed for evaluation based on data gathered in Victoria, Australia. The BRL model comprises a simple exponential correlation [29]:

For any value of M_t

$$I_d = \left(\frac{1}{1 + e^{7.997(M_t - 0.586)}} \right) I_H$$

- **Liu and Jordan's Model**

Liu and Jordan [30] report a correlation based on data collected from different localities in Canada and USA

$$\text{For } 0.75 < M_t \leq 1$$

$$I_d = (0.384 - 0.416M_t)I_H$$

- **Spencer's Model**

Spencer [31] proposed a correlation based on the clearness index with a number of Australian data sets (five different stations).

$$\text{For } 0.35 < M_t \leq 0.75$$

$$I_d = (a_3 - b_3M_t)I_H$$

It assumed that I_d could have constant values beyond the above range of M_t and the coefficients a_3 and b_3 depend on the latitude.

$$a_3 = 0.94 + 0.0118|\varphi|$$

$$b_3 = 1.185 + 0.0135|\varphi|$$

The value of φ is the latitude of the under studied location.

- **Reindl's Model**

The diffuse radiation I_d was estimated on horizontal surfaces indexed at five different locations in Europe and the United States of America by Reindl et al. They developed two different models by values of diffuse and global radiations. The first model (Reindl-1) uses the clearness input data to estimate the diffuse radiation.

$$\text{For } 0 < M_t \leq 0.3 \quad I_d = (1.02 - 0.248M_t)I_H$$

$$\text{For } 0.3 < M_t < 0.78 \quad I_d = (1.45 - 1.67M_t)I_H$$

$$\text{For } 0.78 \leq M_t \leq 1 \quad I_d = (0.147)I_H$$

The second correlation (Reindl-2) estimates the diffuse fraction by taking into account the clearness index M_t and the solar elevation α .

$$\text{For } 0 < M_t \leq 0.3 \quad I_d = (1.02 - 0.254M_t + 0.0123 \sin \alpha)I_H$$

$$\text{For } 0.3 < M_t < 0.78 \quad I_d = (1.4 - 1.749M_t + 0.177 \sin \alpha)I_H$$

$$\text{For } 0.78 \leq M_t \leq 1 \quad I_d = (0.486M_t - 0.182 \sin \alpha)I_H$$

- **Oliveira's Model**

Oliveira et al. [32] suggested a polynomial correlation of fourth order based on collected data from a tropical climate in Sao Paolo, Brazil.

$$\text{For } 0 < M_t \leq 0.17 \quad I_d = (1)I_H$$

$$\text{For } 0.17 < M_t < 0.75 \quad I_d = \left(0.97 + 0.8M_t - 3M_t^2 - 3.1M_t^3 + 5.2M_t^4\right)I_H$$

$$\text{For } 0.75 < M_t \leq 1 \quad I_d = (0.17)I_H$$

- **Soares' Model**

Soares and others [33] used the same data set as Oliveira and suggested a synthetic polynomial correlation of fourth-order utilizing a neural network technique.

$$\text{For } 0 < M_t \leq 0.17 \quad I_d = (1)I_H$$

$$\text{For } 0.17 < M_t < 0.75 \quad I_d = \left(0.9 + 1.1M_t - 4.5M_t^2 - 0.01M_t^3 + 3.14M_t^4\right)I_H$$

$$\text{For } 0.75 < M_t \leq 1 \quad I_d = (0.17)I_H$$

- **Muneer's Model**

Muneer et al. [34] established a correlation for desert and tropical locations, based on data of New Delhi, India.

$$\text{For } 0 < M_t < 0.175 \quad I_d = (0.95)I_H$$

$$\text{For } 0.175 < M_t < 0.755 \quad I_d = \left(0.9698 + 0.4353M_t - 3.4499M_t^2 + 2.1888M_t^3\right)I_H$$

$$\text{For } 0.775 < M_t < 1 \quad I_d = (0.26)I_H$$

The summary of the all parametric models that are based on clearness index is given in Table 2.

Table 2. Summary of the parametric models.

Models	Constraints	Diffuse Fraction (r_d)
Chandrasekaran and Kumar	$0 < M_t \leq 0.24$	$1.0086 - 0.178M_t$
	$0.24 < M_t \leq 0.8$	$0.9686 + 0.1325M_t + 1.4183M_t^2 - 10.1862M_t^3 + 8.3733M_t^4$
	$0.8 < M_t \leq 1$	$1.0086 - 0.178M_t$
Erbs	$0 < M_t \leq 0.22$	$1 - 0.09M_t$
	$0.22 < M_t \leq 0.8$	$0.9511 - 0.1604M_t + 4.388M_t^2 - 16.638M_t^3 + 12.336M_t^4$
	$0.8 < M_t \leq 1$	0.165
Hawladar	$0 < M_t \leq 0.225$	$0.915M_t$
	$0.225 < M_t < 0.775$	$1.135 - 0.9422M_t - 0.3878M_t^2$
	$0.775 \leq M_t \leq 1$	0.215
Jacovides	$0 < M_t \leq 0.1$	0.987
	$0.1 < M_t \leq 0.8$	$0.94 + 0.937M_t - 5.01M_t^2 + 3.32M_t^3$
	$0.8 < M_t \leq 1$	0.177
Karatasou	$0 < M_t \leq 0.78$	$0.9995 - 0.05M_t - 2.4156M_t^2 + 1.4926M_t^3$
	$0.78 < M_t \leq 1$	0.2
Lam and Li	$0 < M_t \leq 0.15$	0.977
	$0.15 < M_t \leq 0.17$	$1.237 - 1.361M_t$
	$0.17 < M_t \leq 1$	0.273
Louche	$0 < M_t \leq 1$	$I_b = (-10.676M_t^5 + 15.307M_t^4 - 5.205M_t^3 + 0.99M_t^2 - 0.059M_t + 0.02)$
Miguel	$0 < M_t \leq 0.21$	$0.995 - 0.081M_t$
	$0.21 < M_t \leq 0.76$	$0.724 + 2.738M_t - 8.32M_t^2 + 4.967M_t^3$
	$0.76 < M_t \leq 1$	0.18
Orgill and Hollands	$0 < M_t < 0.35$	$1 - 0.249M_t$
	$0.35 \leq M_t \leq 0.75$	$1.577 - 1.84M_t$
	$0.75 < M_t \leq 1$	0.177
Boland	For any value of M_t	$\frac{1}{1 + e^{2.9997(M_t - 0.586)}}$
Liu and Jordan	$0.75 < M_t \leq 1$	$0.384 - 0.416M_t$
Spencer	$0.35 < M_t \leq 0.75$	$a_3 - b_3M_t$
Reindl-1	$0 < M_t \leq 0.3$	$1.02 - 0.248M_t$
	$0.3 < M_t < 0.78$	$1.45 - 1.67M_t$
	$0.78 \leq M_t \leq 1$	0.147
Reindl-2	$0 < M_t \leq 0.3$	$1.02 - 0.254M_t + 0.0123 \sin \alpha$
	$0.3 < M_t < 0.78$	$1.4 - 1.749M_t + 0.177 \sin \alpha$
	$0.78 \leq M_t \leq 1$	$0.486M_t - 0.182 \sin \alpha$
Oliveira	$0 < M_t \leq 0.17$	1
	$0.17 < M_t < 0.75$	$0.97 + 0.8M_t - 3M_t^2 - 3.1M_t^3 + 5.2M_t^4$
	$0.75 < M_t \leq 1$	0.17
Soares	$0 < M_t \leq 0.17$	1
	$0.17 < M_t < 0.75$	$0.9 + 1.1M_t - 4.5M_t^2 - 0.01M_t^3 + 3.14M_t^4$
	$0.75 < M_t \leq 1$	0.17
Muneer	$0 < M_t < 0.175$	0.95
	$0.175 < M_t < 0.755$	$0.9698 + 0.4353M_t - 3.4499M_t^2 + 2.1888M_t^3$
	$0.775 < M_t < 1$	0.26

3.2. Hourly Direct Radiation on Horizontal Surface (I_b)

When sunlight travels through the earth's atmosphere, some of it, called beam radiation, strikes the earth's surface, throwing sharp shadows and is undisturbed [35].

Direct normal radiation on horizontal surfaces (I_{bN}) can be measured by an instrument called a pyrhelimeter. Moreover, the direct normal radiation (I_{bN}) can be estimated by the number of models such as: the Bird model [36], METSTAT [37], the Yang model [38], REST2 [39], and the Ineichen model [40].

$$I_b = I_{bN} \cos \theta_z$$

As previously mentioned, global solar radiation is calculated as the sum of diffuse radiation and direct radiation on a horizontal surface. Therefore, direct radiation (I_b) can be computed by the difference between global solar radiation (I_H) and diffuse radiation (I_d) on a horizontal surface.

$$I_b = I_H - I_d$$

3.3. Recognizing Accurate Models to Estimate Diffuse Radiation on Horizontal Surfaces

A few studies have been done on the estimation of diffuse radiation on horizontal surfaces using parametric and decomposition models. For this purpose, diffuse radiation measurements are mostly taken either by a pyranometer fitted with a shadow ball device placed over a sun tracker unit or by a shadow band. In order to find a suitable model for the location concerned, the measured and estimated values are compared against one another.

Recently, a study was done in Southeast Australia to determine the diffuse radiation on a horizontal surface using nine diffuse radiation models [41]. Perez model performance was found to be satisfactory in Southeast Australia.

A case study was done at the Jiading Campus of Tongji University in China to find the most accurate decomposition model for the location concerned [42]. A modified Collares-Pereira and Rabl model, by Gueymard (CPRG model) [43] was the most accurate for the Jiading Campus.

In a test by Kuo et al., fourteen models were used to estimate diffuse radiation on horizontal surfaces in Taiwan. Among the fourteen models considered in the study, those developed by Erbs, Chandrasekaran and Kumar, and Boland et al. performed better [44].

A group of researchers in Algeria evaluated the KTCOR model to get an estimation on diffuse radiation on horizontal surfaces. Moreover, Orgill and Hollands, Liu and Jordan, Reindl, Erbs, and Chendo's [45] models were used to estimate diffuse radiation on horizontal surfaces [46].

In another study, eight unique models were applied to estimate diffuse parts of radiation in view of a database of measurements from Vienna, Austria, and they were compared [47]. For most parts of the work, these models include numerical definitions with numerous coefficients whose values are regularly valid for a particular area. The outcomes suggested that a few models can make moderately reliable estimations of the diffuse fractions of global radiation. The correlation of the eight models on the deduction of the diffuse fraction of horizontal radiation suggests that the calculations of Reindl et al., Orgill and Hollands, and Erbs et al., provide excellent results for Vienna. A summary of studies on identifying the most accurate diffuse models on horizontal surfaces for different locations is given in Table 3.

Table 3. Summary of studies on identifying the most accurate diffuse models for horizontal surfaces.

Authors	Location	Most Accurate Models
N. A. Engerer	Southeast Australia	Perez
Wanxiang Yao et al.	China	Gueymard
Kuo	Taiwan	Erbs, Chandrasekaran and Kumar, and Boland
Chikh et al.	Algeria	KTCOR
Dervishi et al.	Vienna, Austria	Erbs, Reindl, and Orgill and Hollands

4. Hourly Global Solar Radiation on an Inclined Surface (I_{β})

Beam radiation ($I_{b\beta}$), reflected radiation (I_r), and diffuse radiation ($I_{d\beta}$) are the three components of the global solar radiation incident on an inclined surface (I_{β}). The fraction of incident radiation reflected by the ground is called reflected radiation.

$$I_{\beta} = I_{d\beta} + I_{b\beta} + I_r$$

Generally, diffuse radiation models for inclined surfaces can be classified into two groups: isotropic and anisotropic models. They differ in the division of the sky into regions with normal and elevated diffuse radiation intensities. Isotropic models assume there is uniformity in the distribution of diffuse radiation intensity over the sky. Anisotropic models include appropriate modules for representing areas of elevated diffuse radiation.

4.1. Isotropic Models

- **Badescu's Model**

Badescu presented a model for solar diffuse radiation on a sloped surface using the following equation [48]:

$$I_{d\beta} = \left(\frac{3 + \cos(2\beta)}{4} \right) \times I_d$$

- **Koronakis' Model**

Koronakis used an alternative assumption of isotropic sky diffuse radiation, which covers 66.7% of the total sky radiation for a vertical plane oriented southward [49].

$$I_{d\beta} = \frac{1}{3} \left(\frac{1}{2 + \cos \beta} \right) \times I_d$$

- **Liu and Jordan's Model**

Liu and Jordan's model is one of the earliest and simplest models of radiation [50]. This model presumes that diffuse radiation intensity is distributed uniformly over the whole sky, which is calculated as follows:

$$I_{d\beta} = \left(\frac{1 + \cos \beta}{2} \right) \times I_d$$

- **Tian's Model**

Tian proposed the following radiation model [51]:

$$I_{d\beta} = \left(1 - \frac{\beta}{180} \right) \times I_d$$

4.2. Anisotropic Models

- **Bugler's Model**

Bugler (1977) added modules for the diffuse radiation emanating from the sun's disc and alternative components of the sky counting on the sun's angular height over the horizon [52]. Bugler's equation is:

$$I_{d\beta} = \left(\frac{1 + \cos \beta}{2} \left(I_d - 0.05 \frac{I_{b\beta}}{\cos \theta_z} \right) \right) + 0.05 I_{b\beta} \cos \theta$$

- **Temps and Coulson's Model**

Temps and Coulson (1977) modified the isotropic model of Liu and Jordan and introduced two terms that represent diffuse radiation by assuming a clear sky condition [53].

$$I_{d\beta} = \frac{1}{2} I_d (1 + \cos \beta) P_1 P_2$$

where P_1 is the vicinity of the sun's disc and P_2 is the sky radiation from the region near the horizon.

$$P_1 = 1 + \cos^2 \theta (\sin^3 \theta_z)$$

$$P_2 = 1 + \sin^3 \left(\frac{\beta}{2} \right)$$

- **Hay's Model**

Another anisotropic model is the one proposed by Hay and Davies, which is commonly referred to as the Hay model. Two primary sources are assumed to be the origins of sky diffuse radiation,

namely the disc of the sun disc and the rest of the sky with isotropic diffuse radiation [54]. The two components are described by the anisotropy index f_{Hay} :

$$f_{Hay} = \frac{I_b}{I_0} = \frac{I_H - I_d}{I_0}$$

Based on the Hay model, the equation for the intensity of diffuse radiation on an inclined plane has the form

$$I_{d\beta} = I_d \left[f_{Hay} \left(\frac{\cos \theta}{\cos \theta_z} \right) + \left(\frac{1 + \cos \beta}{2} \right) (1 - f_{Hay}) \right]$$

- **Reindl's Model**

Reindle [55] proposed a model for the diffuse radiation emitted from the areas near the horizon line described by the Hay model. Reindle found that with increasing overcast sky, there is a decrease in the diffuse radiation intensity originating from the given region. Therefore, the modulating function f_R was included in the module:

$$f_R = \sqrt{\frac{I_b}{I_H}}$$

The Reindl equation is:

$$I_{d\beta} = I_d \left[f_{Hay} \left(\frac{\cos \theta}{\cos \theta_z} \right) + \left(\frac{1 + \cos \beta}{2} \right) (1 - f_{Hay}) \left(1 + f_R \sin^3 \left(\frac{\beta}{2} \right) \right) \right]$$

- **Klucher's Model**

Anisotropic model of Klucher's is based on the models by Temps and Coulson and and Liu and Jordan [56]. Klucher found that Liu and Jordan's isotropic model provides fruitful results for overcast skies but overlooks radiation for some sky conditions, such as partly overcast and clear skies. Such conditions are distinguishable by a rising intensity in the proximity of the circumsolar sky and horizon region. To overcome such a limitation, the Temps and Coulson model was refined by introducing a function f_k that determines the degree of cloud cover.

$$f_k = 1 - \left(\frac{I_d}{I_H} \right)^2$$

- **Klucher's Model Is Described by the Following Equation:**

$$I_{d\beta} = I_d \left[\frac{1}{2} \left(1 + \cos \left(\frac{\beta}{2} \right) \right) \right] \left[1 + f_k \cos^2 \theta \left(\sin^3 \theta_z \right) \right] \left[1 + f_k \sin^3 \left(\frac{\beta}{2} \right) \right]$$

- **The HDKR Model (the Klucher and Reindl, and Hay and Davies' Model)**

The HDKR model was developed with the aim of analyzing the beam reflection and all diffuse radiation terms, such as isotropic, circumsolar, and horizon brightening, by adding them to the solar radiation equation. Although originating from the Hay and Davies model, HDKR introduces the term "horizon brightening" similar to Klucher. As a result, this model was named HDKR (Hay, Davies, Klucher, Reindl) by Duffie and Beckman [10].

$$I_{d\beta} = I_d \left[\left(\frac{1 + \cos \beta}{2} \right) (1 - f_{Hay}) \left(1 + f_R \sin^3 \left(\frac{\beta}{2} \right) \right) \right]$$

- **Skartveit and Olseth's Model**

Solar radiation measurements carried out by Skartveit and Olseth in Bergen (Norway) partly indicated the fact that sky diffuse radiation originates from the part of the sky surrounding the

zenith under overcast sky conditions. This effect disappears with the disappearance of cloud cover. To overcome this effect, Skartveit and Olseth refined Hay's model [57].

$$I_{d\beta} = I_d \left[\left(f_{Hay} \left(\frac{\cos \theta}{\cos \theta_z} \right) \right) + (1 - f_{Hay} - Z) \left(\frac{1 + \cos \beta}{2} \right) - S(\omega, \Omega_i) \right]$$

where Z is the correcting factor.

$$Z = 0.3 - 2f_{Hay} \text{ for } f_{Hay} < 0.15$$

$$Z = 0 \text{ for } f_{Hay} \geq 0$$

The effect of barriers blocking the horizon and obscuring part of the diffuse radiation incident on a sloped plane, is represented by the term $S(\omega, \Omega_i)$. This term is usually neglected as data are typically derived from radiometric stations. Situated in open terrains, radiometric stations face insignificant natural or artificial obstacles [2].

- **Steven and Unsworth's Model**

The anisotropic model of Steven and Unsworth is defined as diffuse radiation on a plane inclined at a β angle. The source is considered to be the heliocentric radiation of the gleaming horizon and the sun's disk.

$$I_{d\beta} = I_d \left[\left(0.51 \left(\frac{\cos \theta}{\cos \theta_z} \right) \right) + \left(\frac{1 + \cos \beta}{2} \right) - \frac{1.74}{1.26\pi} \left\{ \sin \beta - \beta \frac{\pi}{180} \cos \beta - \pi \sin^2 \frac{\beta}{2} \right\} \right]$$

- **Wilmott's Model**

Another anisotropic model is Willmott's model, which adapted the model proposed by Hay and defined a new anisotropy index [58].

$$I_{d\beta} = I_d \left[\frac{I_{bN} R_b}{I_{sc}} + C_\beta \left(1 - \frac{I_{bN}}{I_{sc}} \right) \right]$$

$$I_{bN} = \frac{I_b}{\cos \theta_z}$$

where $C_\beta = 1.0115 - 0.20293\beta - 0.080823\beta^2$ and β is in radians, and I_{sc} is the solar constant.

- **Perez' Model**

The basis of the Perez model is an in-depth applied mathematic analysis of the sky's diffuse components. This model divides diffuse radiation into three components: isotropic background, circumsolar, and horizon zones [59]. The governing equation is:

$$I_{d\beta} = I_d \left[\frac{1 + \cos \beta}{2} (1 - F_1) + F_1 \frac{a_1}{a_2} + F_2 \sin \beta \right]$$

In this equation a_1 and a_2 represent solid angles occupied by the circumsolar region, weighted by its average incidence radiation on an angled and horizontal surface, respectively; F_2 and F_1 , are the dimensionless horizon brightness and the the circumsolar coefficients respectively. The two factors are defined as follows:

$$a_1 = \max(0, \cos \theta)$$

$$a_2 = \max(\cos 85^\circ, \cos \theta_z)$$

These increasing factors set the radiation magnitude values within the two anisotropic regions relevant to those in the major a part of dome. Within the model, the degree of anisotropy could

be a performance of solely these two regions. Thus, the model will perform both as an isotropic configuration ($F_1 = F_2 = 1$), and collectively incorporating circumsolar and/or horizon brightening equivalent time.

$$F_1 = \max\left\{0, \left[F_{11} + F_{12}\Delta + F_{13}\theta_z\left(\frac{\pi}{180}\right)\right]\right\}$$

$$F_2 = \left[F_{12} + F_{22}\Delta + F_{23}\theta_z\left(\frac{\pi}{180}\right)\right]$$

$$\Delta = m \frac{I_d}{I_o}$$

$$m = \frac{1}{\cos \theta_z}$$

here m is the air mass (dimensionless), I_d is the hourly diffuse radiation on a horizontal surface and I_o is the extraterrestrial radiation at normal incidence (W/m^2). The ϵ is a function of hourly diffuse radiation I_d which is given in Table 4 and direct beam radiation I_b [60]. The required coefficients $F_{i,j}$ are obtained from Perez et al., as seen in Table 5.

$$\epsilon = \frac{\frac{I_d + I_b}{I_d} + 5.535 \times 10^{-6} \theta_z^3}{1 + 5.535 \times 10^{-6} \theta_z^3}$$

Table 4. Discrete sky clearness categories [60].

ϵ	Lower Range	Upper Range
1 Overcast	1	1.065
2	1.065	1.230
3	1.230	1.500
4	1.500	1.950
5	1.950	2.800
6	2.800	4.500
7	4.500	6.200
8 Clear	6.200	∞'

Table 5. Brightness coefficients for the Perez Anisotropic Sky [60].

ϵ Bin	F_{11}	F_{12}	F_{13}	F_{21}	F_{22}	F_{23}
1.000	−0.008	0.588	−0.062	−0.060	0.072	−0.022
1.065	0.130	0.683	−0.151	−0.019	0.066	−0.029
1.230	0.330	0.487	−0.221	0.055	−0.064	−0.026
1.500	0.568	0.187	−0.295	0.109	−0.152	0.014
1.950	0.873	−0.392	−0.362	0.226	−0.462	0.001
2.800	1.132	−1.237	−0.412	0.288	−0.823	0.056
4.500	1.060	−1.600	−0.359	0.264	−1.127	0.131
6.200	0.678	−0.327	−0.250	0.159	−1.377	0.251

The details and mathematical relationships of diffuse models on inclined surfaces including isotropic and anisotropic models are provided in Table 6.

Table 6. Summary of diffuse models on inclined surfaces.

Models	Diffuse Radiation on Inclined Surfaces (I_{dfi})
Badescu	$\left(\frac{3+\cos(2\beta)}{4}\right) I_d$
Koronakis	$\frac{1}{3} \left(\frac{1}{2+\cos\beta}\right) I_d$
Liu and Jordan	$\left(\frac{1+\cos\beta}{2}\right) I_d$
Tian	$\left(1 - \frac{\beta}{180}\right) I_d$
Bugler	$\left(\frac{1+\cos\beta}{2} \left(I_d - 0.05 \frac{I_{b\beta}}{\cos\theta_z}\right)\right) + 0.05 I_{b\beta} \cos\theta$
Temps and Coulson	$\frac{1}{2} I_d (1 + \cos\beta) P_1 P_2$
Hay	$I_d \left[f_{Hay} \left(\frac{\cos\theta}{\cos\theta_z}\right) + \left(\frac{1+\cos\beta}{2}\right) (1 - f_{Hay}) \right]$
Reindl	$I_d \left[f_{Hay} \left(\frac{\cos\theta}{\cos\theta_z}\right) + \left(\frac{1+\cos\beta}{2}\right) (1 - f_{Hay}) \left(1 + f_R \sin^3\left(\frac{\beta}{2}\right)\right) \right]$
Klucher	$I_d \left[\frac{1}{2} \left(1 + \cos\left(\frac{\beta}{2}\right)\right) \right] \left[1 + f_k \cos^2\theta (\sin^3\theta_z)\right] \left[1 + f_k \sin^3\left(\frac{\beta}{2}\right)\right]$
HDKR	$I_d \left[\left(\frac{1+\cos\beta}{2}\right) (1 - f_{Hay}) \left(1 + f_R \sin^3\left(\frac{\beta}{2}\right)\right) \right]$
Skartveit and Olseth	$I_d \left[\left(f_{Hay} \left(\frac{\cos\theta}{\cos\theta_z}\right)\right) + (1 - f_{Hay} - Z) \left(\frac{1+\cos\beta}{2}\right) - S(\omega, \Omega_i) \right]$
Steven and Unsworth	$I_d \left[\left(0.51 \left(\frac{\cos\theta}{\cos\theta_z}\right)\right) + \left(\frac{1+\cos\beta}{2}\right) - \frac{1.74}{1.26\pi} \left\{ \sin\beta - \beta \frac{\pi}{180} \cos\beta - \pi \sin^2\left(\frac{\beta}{2}\right) \right\} \right]$
Willmott	$I_d \left[\frac{I_{bN} R_b}{I_{sc}} + C_\beta \left(1 - \frac{I_{bN}}{I_{sc}}\right) \right]$
Perez	$I_d \left[\frac{1+\cos\beta}{2} (1 - F_1) + F_1 \frac{a_1}{a_2} + F_2 \sin\beta \right]$

4.3. Recognizing Accurate Models for Estimation of Diffuse Radiation on Angled Surfaces

A number of researchers have attempted to find the most accurate models among anisotropic and isotropic models for estimating diffuse solar radiation on oblique surfaces. To find the most suitable model for a specific location, the amount of estimated diffuse radiation on an inclined surface at various angles is compared with the value of the diffuse radiation on an angled surface measured by a pyranometer with a shadow band at the same angle.

New models for estimation of diffuse solar radiation on an inclined surface were suggested by the Laboratory of Solar Radiometry of Botucatu-UNESP (latitude 22°9' S, longitude 48°45' W) in Brazil. The results of the proposed models were compared with some isotropic and anisotropic model results. The results indicated that the isotropic and anisotropic models were more accurate than the proposed models [61].

A study was done in Singapore, at 1°37' N, 103°75' E. The values of radiation sensors facing 60° NE, tilted at 10°, 20°, 30°, and 40° and vertically tilted radiation sensors facing south, north, west, and east in Singapore were measured. A pyranometer with a shadow band measured the diffuse horizontal radiation while another pyranometer measured the global radiation on a horizontal surface. The direct radiation value on a horizontal surface was calculated using the difference between global radiation on a horizontal surface and diffuse horizontal radiation. The diffuse radiation was calculated for an inclined surface using an isotropic model (Liu and Jordan's model) and two anisotropic models (Klucher and Perez' models) and was compared with the measured values. The model of Perez et al. was proposed as the best model for Singapore [62].

In a study conducted by the Royal Meteorological Institute of Belgium in UCCLE (latitude 50.79° N, longitude 4.35° E) the diffuse solar radiation on an inclined surface was measured by three isotropic models (Liu and Jordan, Korokanis, Badescu) and 11 anisotropic models (Bugler, Hay, Skartveit and Olseth, Willmott, Reindl, Temps and Coulson, Klucher, Perez, Iqbal, Muneer and Gueymard). The data collected over a period of eight months (April 2011 to November 2011) were

utilized to define the relative capacity of 14 different models to estimate the global solar radiation on an inclined surface facing south as a distinctive element of sky conditions. It was identified that Bugler's model performed the most effectively under all sky conditions, such as partly clear and clear, while Willmott's model was observed to provide the most accurate results under overcast and partly cloudy conditions. Finally, Perez' model most closely fit the estimation under overcast conditions [4].

In a study conducted by Gulin et al. at the University of Zagreb (45°80' N, 15°87' E), global radiation on a horizontal surface was measured using a pyranometer, while direct radiation was measured by a sun tracker pyrheliometer with an extra sensor for closed-loop tracking of the sun. Three isotropic models (Liu and Jordan, Korokanis and Badescu) and six anisotropic models (Skartveit and Olseth, Willmott, Temps and Coulson, Bugler, Hay and Klucher) were used to estimate solar diffuse radiation on an inclined surface at 5°, 30°, 55°, and 80°. Gulin et al. developed three different neural network models for predicting the solar radiation incident on an oblique surface. These models' performance was then evaluated in light of the three isotropic and six anisotropic rival models for tilted surfaces [63].

In Botucatu region of the state of São Paulo, Brazil (22°53' S, 48°26' W), twenty models were used to estimate the hourly diffuse radiation incident on angled surfaces facing north at and 32.85°, 22.85°, and 12.85°, under various cloudy conditions. The most promising results were obtained using the anisotropic models of Ma and Iqbal, Hay, Reindl et al., and Willmott, while the circumsolar models and the isotropic models of Badescu and Koronakis proved to be the best [64].

In a study carried out in Poland, Polish researchers selected numeric models of both isotropic and anisotropic nature for estimation of the diffuse solar radiation on photovoltaic module planes. They clarified which model was most appropriate for central Poland. Isotropic models (Liu-Jordan, Badescu, Koronakis, Tian) and anisotropic models (Hay, Steven and Unsworth) were used to estimate the distribution of radiation power on photovoltaic planes slanted at 30°, 45°, and 60° facing south. The outcomes demonstrated that the anisotropic models facilitated obtaining higher radiation throughout the year in comparison to isotropic models for the Polish latitude [65].

Włodarczyk and Nowak carried out a study and statistically analyzed 14 major models for the solar radiation intensity on an inclined plane. Models with various degrees of complexity were analyzed, from the simplest classical isotropic model to the most complex anisotropic model (the Perez model). They compared the model results with data collected at 35° and 50° angles from the actinometrical station laboratory in Wrocław, Poland. The analyzed models of diffuse solar radiation [66].

A research done in Egypt suggested that the Perez model is suitable for that area. This model was selected among the Temps and Coulson, Bugler and Perez models [67]. Another comparative study addressed the performance of one isotropic and nine anisotropic models, where actual data were employed to estimate the solar radiation diffusion of inclined surfaces. The data were obtained from the province of Valladolid, Spain, on a south-facing surface inclined at 42°. It became clear that the best model was Hay's, followed by Muneer and Willmott's models [68]. Based on a daily analysis, Perez' model and the isotropic model showed an average performance and the Temps-Coulson model had the least satisfying results.

Mehleri et al. [69] developed a new neural network model (RBF) to estimate diffuse radiation on inclined surfaces for the Athens region. The RBF model was suggested as the most accurate model for the location.

A summary of studies on identifying the most accurate diffuse models on inclined surfaces for different locations is given in Table 7.

Table 7. Summary of studies on finding the most accurate diffuse models for inclined surfaces.

Authors	Location	Most Accurate Models
Dal Pai et al.	Brazil	Isotropic and anisotropic models
Khoo et al.	Singapore	Perez
Demain et al.	Belgium	Willmott, Perez
Gulin et al.	Croatia	3 different neural network models
Souza and Escobedo	Brazil	Iqbal, Hay, Reindl, Willmott, Badescu and Koronakis
Frydrychowicz-Jastrzebska and Bugala	Poland	Hay, Steven and Unsworth
Włodarczyk and Nowak	Poland	Reindl, Gueymard, Perez, Koronakis and Muneer [70]
Elminir et al.	Egypt	Perez
Diez-Mediavilla et al.	Spain	Hay, Muneer and Willmott
Mehleri et al.	Athens	RBF model

4.4. Estimating Direct Beam Radiation of an Angled Surface ($I_{b\beta}$)

Based on results by Iqbal, direct beam radiation value on an angled surface can be calculated using the following equation [6]:

$$I_{b\beta} = r_b I_b$$

where r_b is the ratio of hourly radiation received by an angled surface to that of a horizontal surface outside the earth's atmosphere.

$$r_b = \frac{I_{0\beta}}{I_0} \approx \frac{\cos\theta}{\cos\theta_z}$$

where θ_0 is the angle of incidence of an equator facing surface in degrees, and θ_z is the zenith angle, which is defined as the angle between the sun and the Pole of the Horizontal Coordinate System, in degrees. Figure 4 shows a diagram of the equality of angles θ_0 and θ_z .

$$\cos\theta_z = \sin\delta \sin\varphi + \cos\delta \cos\varphi \cos\omega$$

$$\cos\theta_0 = \sin\delta \sin(\varphi - \beta) + \cos\delta \cos(\varphi - \beta) \cos\omega$$

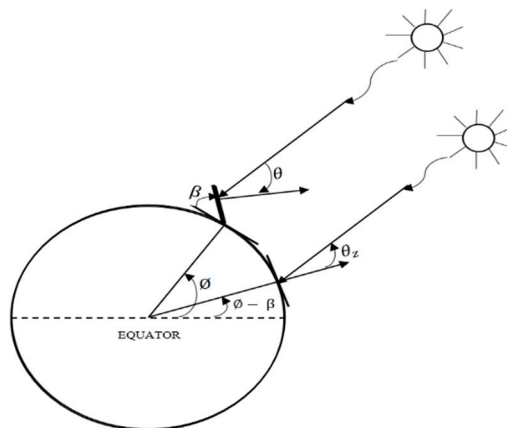


Figure 4. Diagram of the equality of angles θ and θ_z , adapted with permission from Liu and Jordan [50].

The mathematic relation for the incidence angle θ is given by the following equation for surfaces aligned in any direction with respect to the local meridian [6,71]:

$$\begin{aligned} \cos\theta = & (\sin\varphi \cos\beta - \cos\varphi \sin\beta \cos\gamma) \sin\delta \\ & + (\cos\varphi \cos\beta + \sin\varphi \sin\beta \cos\gamma) \cos\delta \cos\omega + \cos\delta \sin\beta \sin\gamma \sin\omega \end{aligned}$$

4.5. Estimating Ground-Reflected Radiation on an Angled Surface (I_r)

Part of the global solar radiation that is reflected by the earth's surface and any other intercepting object is called ground-reflected radiation.

$$I_r = I_H \rho \left(\frac{1 - \cos \beta}{2} \right)$$

Determining the appropriate albedo is the main concern of users modeling this component, where ρ is the ground albedo [72]. Throughout the day, the ground albedo varies due to several factors, such as deviations from Lambert's law of isotropy and variations in ground properties (e.g., snow cover or soil water content). This is also true for dry ground albedo, with minimal alterations around noon. Furthermore, due to the possibility of partial shading as well as azimuthal inhomogeneities in ground cover, albedos of the morning and afternoon are not symmetrical. In addition, the albedos for the early morning hours and also the late evening hours are usually close to 1 or 0. This is mainly because of artefacts like shading or instrumental cosine error. The ground albedo is often estimated at a constant 0.2 value [73].

4.6. Combination of Diffuse Estimation Models for Horizontal and Inclined Surfaces

As previously explained, to measure diffuse radiation received by a horizontal surface, a diffuse shadow band on the horizontal surface or a pyrheliometer is compulsory. Furthermore, to measure diffuse radiation on an inclined surface, a diffuse shadow band is necessary. The values of direct or diffuse radiation are measured infrequently at meteorological stations, while the global radiation values on horizontal surfaces are usually available. Considering the above-mentioned limitations, some researchers have used combinations of diffuse models for horizontal surfaces, whether decomposition or parametric models and diffuse models for an inclined surface, or isotropic or anisotropic models. Finally, the estimated global radiation values on inclined surfaces are compared with the measured global radiation values on inclined surfaces.

A group of researchers in Bhopal, India, used a decomposition model in order to determine the diffuse radiation on a horizontal surface. They also used three isotropic and three anisotropic models to calculate diffuse radiation on a sloped surface. They found that Badescu's model is the best isotropic model for India [74].

More recently, a study was done in the south of Sindh region, Pakistan, to find the best combination of models for diffuse radiation received by horizontal and angled surfaces. To achieve this objective, nine new models were developed based on function of clearness index models [75,76] Erbs' model [21], Liu and Jordan's model [30], a cubic polynomial model and a quadratic polynomial model [76], a sunshine fraction model (Barbara's model) [77], and Haydar et al.'s model [78] in order to estimate diffuse radiation on a horizontal surface and an isotropic model to estimate diffuse radiation on an inclined surface [79]. The calculated and measured values showed that the best is a combination of the sunshine fraction model with Liu and Jordan's model [80].

In South Korea, a study was conducted with the objective of predicting solar irradiation on inclined surfaces in reference to horizontal measurements. This study included measurements of the accuracy of the two established models. Using the first and second types of models, respectively, diffuse horizontal radiation from global components and global radiation on angled planes from diffuse and global components on horizontal surfaces were quantified. The solar radiation was gradually reduced as the inclined angle was increased from horizontal to vertical surfaces, apart from south-facing orientations. The maximum value was observed at inclination angles between 20° and 40° [81].

In a case study carried out in Karaj, Iran, combinations of a decomposition model (Miguel et al.) and 12 models including four isotropic models (Badescu, Koronakis, Tian, and Liu and Jordan), and some anisotropic models (Reindl, Skartveit and Olseth, Hay, Steven and Unsworth, Temps and

Coulson, Klucher and Perez) were investigated. The results indicated that the Skartveit and Olseth, Hay, Reindl, and Perez models made the most accurate predictions for south-facing surfaces [82].

A similar research was done to quantify the level of accuracy of different models. The first type consisted of seven diffuse radiation models for a horizontal surface. The second type with fifteen models differentiated between measurements of global radiation on inclined planes and global components on horizontal surfaces. The study combined two model classes and calculated the level of adequacy of each association for the data, which was collected hourly at Ajaccio, a French Mediterranean site. The result of each combination was compared with the value of data collected on 45° and 60° tilted surfaces. The best combination was Maxwell + Klucher for the 45° inclination angle. For 60° inclination, the most efficient model was Skartveit and Olseth's model combined with Klucher's model [83].

A study was done in Padova, Italy, to find the best model for estimating diffuse radiation on horizontal and tilted surfaces. To reach this goal, four decomposition models were used to estimate diffuse radiation on horizontal surfaces, and an isotropic model and three anisotropic models were used to estimate diffuse radiation on tilted surfaces. Erbs, Perez, Erbs and HDKR were suggested as the best combination [84]. A summary of studies on identifying the most accurate combination models to estimate diffuse radiation on horizontal and inclined surfaces for different locations is given in Table 8.

Table 8. Summary of studies on finding the most accurate diffuse models for horizontal and inclined surfaces.

Authors	Location	Most Accurate Models for Horizontal and Inclined Surfaces
Shukla et al.	India	Decomposition model + Badescu
Farhan et al.	Pakistan	Sunshine fraction model + Liu and Jordan's model
Lee et al.	South Korea	CIBSE Guide J [85] + Isotropic
Noorian et al.	Iran	Skartveit and Olseth, Hay, Reindl and Perez
Notton et al.	French	Maxwell + Klucher
Padovan and Col	Italy	Erbs+ Perez, Erbs + HDKR

5. Estimation of Daily Global Solar Radiation on a Horizontal Surface (H_H)

Daily global radiation on a surface is the average of the hourly global radiation on a surface that may be found with the following equation [6]:

$$H_H = H_b + H_d$$

where H_H is the daily global radiation on a horizontal surface, H_b is the beam radiation on a horizontal surface and H_d is the diffuse radiation on a horizontal surface.

$$K_t = \frac{H_H}{H_o}$$

H_o is daily extraterrestrial radiation ($\text{KJm}^{-2}\cdot\text{day}^{-1}$), which is found with the following equation:

$$H_o = \frac{24 \times 3.6}{\pi} I_{sc} E_0 \left[\left(\frac{\pi}{180} \right) w_s (\sin \delta \sin \varphi) + (\cos \delta \cos \varphi \sin w_s) \right]$$

where E_0 is the eccentricity correction factor, w_s is the sunrise hour angle, δ is the declination angle, and φ is the latitude.

$$w_s = \cos^{-1}(-\tan \varphi \tan \delta)$$

Then the value of H_d is calculated by one of the models defined in Section 3.1.2.

5.1. Daily Radiation on an Inclined Surface (H_β)

The daily global radiation on an inclined surface can be found with the following equation:

$$H_\beta = H_{b\beta} + H_{d\beta} + H_r$$

where $H_{b\beta}$ is the daily beam radiation on an inclined surface, $H_{d\beta}$ is the daily diffuse radiation on an inclined surface that can be calculated by the isotropic and anisotropic models, and H_r is the daily reflected radiation on an inclined surface.

$$H_{b\beta} = R_b H_b$$

$$R_b = \frac{\left(\frac{\pi}{180}\right) w'_s \sin \delta \sin(\varphi - \beta) + \cos \delta \cos(\varphi - \beta) \sin w'_s}{\left(\frac{\pi}{180}\right) w_s \sin \delta \sin \varphi + \cos \delta \cos \varphi \sin w_s}$$

where w'_s is the sunset hour angle for an inclined surface (in degrees) and is given by

$$w'_s = \min\left\{w_s, \cos^{-1}[-\tan \delta \tan(\varphi - \beta)]\right\}$$

5.2. Estimation of the Monthly Average Daily Global Radiation on an Inclined Surface

To estimate the monthly average daily global radiation on an inclined surface, it must be measured on a specific day each month. Klein recommended the average day for each month as can be seen in Table 9 [86].

Table 9. Average day for each month as recommended by Klein [68].

Month	Date	Day of the Year
January	17 January	17
January	16 January	47
January	16 January	75
April	15 April	105
May	15 May	135
June	11 June	162
July	17 July	198
August	16 August	228
September	15 September	258
October	15 October	288
November	14 November	318
December	10 December	344

5.3. Optimum Tilt Angle (β)

Efficiency of a PV panel is highly dependent on the amount of solar radiation received by the PV panel surface. In actuality, the tilt of a solar panel unequivocally influences the gathered yield measurement. This way, solar panels must be inclined at ideal angles in order to gather the most extreme solar energy accessible in particular locations. The most effective technique to improve solar panel tilt is to apply a dynamic sun tracker. Dynamic sun trackers are electromechanical or mechanical devices that continually change the tilt of a solar panel/solar array periodically during the day. On the other hand, the pitfalls of such a system include high capital and wasted energy through the tracking process. Along these lines, changing the tilt angle from daily to monthly for a PV panel may be more attainable than applying a dynamic sun tracker [87]. Estimating the solar radiation on inclined surfaces is a compulsory aspect in the tilt angle selection, which consequently determines the amount of solar radiation received by the PV module surfaces.

Each location has a specific tilt angle that differs from other locations, because one of the factors that highly affects tilt angle values is the latitude of the location. A few researchers around the world have calculated the tilt angle value for different cities. The calculated monthly and annual tilt angle values are given in Table 10.

Table 10. Optimum tilt angle for different locations.

Author	Location (Latitude Longitude)	Monthly Tilt Angle (Degree)	Annual Tilt Angle (Degree)	Orientation	Estimation Diffuse Model for Horizontal and Inclined Surface	
Sinha [88]	Hamirpur, India (31°59' N, 76°52' E)	0 and 60	29.25	south-facing	Erbs model	
Farhan et al. [80]	Sindh, Pakistan (25°12' N, 67°64' E)	spring: 21, summer: 0, autumn: 18, winter: 46	23	south-facing	Sunshine fraction model Liu and Jordan model	
Khorasanizadeh et al. [89]	Tabass, Iran (33°36' N, 51°21'75' E)	62, 53, 38	32	south-facing	Reindl model	
		19, 2, 0				
		0, 12, 32				
		49, 60, 64				
Jafarkazemi and Saadabadi [90]	Abu Dhabi, UAE (24°45' N, 54°37' E)	50, 39, 25	2	south-facing	Klein and Theilacker (KT model) [91]	
		10, 3, 9				
		6, 5, 20				
		36, 48, 52				
Bakirci [92]	Turkey (8 provinces)	optimum tilt angle changed between 0 and 65	-	south-facing	Liu and Jordan	
	Ankara					Ankara: 31.21
	Diyarbakir					Diyarbakir: 32.71
	Erzurum					Erzurum: 32.61
	Istanbul					Istanbul: 34.31
	Izmir					Izmir: 32.61
	Samsun					Samsun: 32.81
Trabzon	Trabzon: 33.21					
Ertekin et al. [93]	Antalya	For autumn: $\phi - 3.41$ For winter: $\phi + 8.14$ For spring: $\phi - 23.92$ For summer: $\phi - 35.17$	For throughout the Turkey: $\phi - 17.31$	south-facing	Liu and Jordan	
	Edirne					
	Hakkari					
	Izmir					
	Sanliuifa					
Zhao [94]	Singapore (1.3667 N, 103.8 E)	27.1, 18.1, 3.4	-	southwest facing	ARMA model [95]	
		0.1, 0.1, 0.1				
		0.1, 0.1, 0.1				
		12.5, 23.3, 28.7				
Maru [96]	Jodhpur, India	49.8, 40.20, 27, 9, 0, 0	31.80	south-facing	Liu and Jordan	
		0, 3.60, 21.6				
Khatib [5]	Malaysia, 5 cities	-	-	-	Liu and Jordan	
	Kuala Lumpur,					29, 19, 5, 0, 0, 0, 0, 0, 14, 24, 24
	Johor Bharu,					24, 17, 3, 0, 0, 0, 0, 0, 11, 22, 23
	Ipoh,					28, 19, 6, 0, 0, 0, 0, 2, 13, 22, 25
	Kuching					19, 16, 3, 0, 0, 0, 0, 0, 11, 21, 22
	Alor Setar					32, 22, 8, 0, 0, 0, 0, 2, 15, 26, 31
Kazem [97]	Sohar, Oman (24°20' N, 56°40' E)	57, 48, 32	-	-	Liu and Jordan	
		10, 0, 0				
		0, 3, 25				
		44, 55, 60				
Ismail [98]	Ramallah, Palestinian (31.8 N, 35.45 E)	Change between 6.5 and 62.6 from June to December	32.8	-	Jain model [99]	
Despotovic [100]	Belgrade, Serbia (44.8 N, 20.46 E)	Average of optimum monthly tilt angle is 43.55	39.9	south-facing	Liu and Jordan	

6. Conclusions

In this paper, a number of well-known models for the purpose of estimation of solar radiation components on horizontal and inclined surfaces were reviewed. As is mentioned in the literature, diffuse radiation models are strongly affected by the location's latitude, therefore finding the most accurate model to estimate the diffuse radiation on horizontal and inclined surfaces in the location under study is necessary. To identify an accurate model for estimating global solar radiation on an inclined surface, the measured and estimated radiation values must be compared. Researchers normally use hourly data to identify the accurate model, while to find the optimum tilt angle, average daily radiation is normally used. Among isotropic models for estimating diffuse radiation on inclined surfaces, the two models that are found to be the most accurate are the Liu-Jordan and Koronakis models. While among anisotropic models, the Perez, Temps-Coulson, Klucher and Bugler models are found to be the most accurate.

The efficiency of a PV panel can be optimized if the panel is positioned in such a way that it receives the maximum amount of incident solar radiation. Solar tracking mechanism will do the job but there are limitations such as costs and wastage of energy. Therefore, there have been a number of works on finding suitable tilt angles which provide a more effective and cheaper solution. This paper summarizes the tilt angles suggested by researchers from different countries and provides a guideline for future reference.

Acknowledgments: Thanks, are also due to Nimehchisalem of the Faculty of Educational Studies, Universiti Putra Malaysia for providing support in language editing of the manuscript.

Author Contributions: Seyed Abbas Mousavi Maleki, designed and developed the main parts of the research work and also mainly responsible for preparing the paper. Associate H. Hizam, contributed of data analysis and writing part and actively contributed to finalize the manuscript. Chandima Gomes, supported in resolving problems with data analysis and structuring of the paper.

Conflicts of Interest: The authors declare no conflict of interest.

Nomenclature

ST	Local solar time
LT	Local standard time
L_s	Standard meridian for a local zone
L_L	Longitude of the location under study in degrees
ET	Equation of time
I_0	Hourly extraterrestrial solar radiation on horizontal surface
I_{sc}	Solar constant
E_0	Eccentricity correction factor
I_H	Hourly global solar radiation on horizontal surface
I_b	Hourly direct beam solar radiation on horizontal surface
I_{bN}	Hourly direct normal beam radiation on horizontal surface
I_d	Hourly diffuse solar radiation on horizontal surface
M_t	Hourly clearness index
I_β	Hourly global solar radiation on inclined surface
$I_{d\beta}$	Hourly diffuse solar radiation on inclined surface
P_1	Vicinity of the sun's disc
P_2	Sky radiation from the region near the horizon
Z	Correcting factor
m	Air mass
$I_{b\beta}$	Hourly direct beam solar radiation on inclined surface
I_r	Hourly ground reflected radiation on inclined surface
H_H	Daily global radiation on a horizontal surface
H_b	Beam radiation on a horizontal surface
H_d	Diffuse radiation on a horizontal surface

K_t	Daily clearness index
w_s	Sunrise hour angle
H_β	Daily global radiation on an inclined surface
$H_{b\beta}$	Daily beam radiation on an inclined surface
$H_{d\beta}$	Daily diffuse radiation on an inclined surface
H_r	Daily reflected radiation on an inclined surface
w'_s	Sunset hour angle
n	The number of the day in the year
Greek Symbols	
β	Tilt angle
θ	Angle of incidence for a surface facing the equator in degrees
θ_z	Zenith angle
δ	Declination angle
Γ	The day angle in radians
ω	Hour angle
γ	Solar azimuth angle
φ	Latitude
ε	Function of hourly diffuse radiation

References

1. Gueymard, C.A. A review of validation methodologies and statistical performance indicators for modeled solar radiation data: Towards a better bankability of solar projects. *Renew. Sustain. Energy Rev.* **2014**, *39*, 1024–1034. [[CrossRef](#)]
2. El-Sebaei, A.A.; Al-Hazmi, F.S.; Al-Ghamdi, A.A.; Yaghmour, S.J. Global, direct and diffuse solar radiation on horizontal and tilted surfaces in Jeddah, Saudi Arabia. *Appl. Energy* **2010**, *87*, 568–576. [[CrossRef](#)]
3. Koussa, M.; Saheb-koussa, D.; Hamane, M. Effect of a daily flat plate collector orientation change on the solar system performances. In Proceedings of the IEEE 7th International Renewable Energy Congress (IREC), Hammamet, Tunisia, 22–24 March 2016.
4. Demain, C.; Journée, M.; Bertrand, C. Evaluation of different models to estimate the global solar radiation on inclined surfaces. *Renew. Energy* **2013**, *50*, 710–721. [[CrossRef](#)]
5. Khatib, T.; Mohamed, A.; Mahmoud, M.; Sopian, K. Optimization of the Tilt Angle of Solar Panels for Malaysia. *Energy Sources A Recover. Util. Environ. Eff.* **2015**, *37*, 606–613. [[CrossRef](#)]
6. Iqbal, M. *An Introduction to Solar Radiation*; Academic Press: Toronto, ON, Canada, 1983.
7. Spencer, J.W. Fourier series representation of the position of the sun. *Appl. Opt.* **1971**, *10*, 2569–2571.
8. Taşdemiroğlu, E. *Solar Energy Utilization Technical and Economic Aspects*; Middle East Technical University: Ankara, Turkey, 1988.
9. Wong, L.T.; Chow, W.K. Solar radiation model. *Appl. Energy* **2001**, *69*, 191–224. [[CrossRef](#)]
10. Duffie, J.A.; Beckman, W.A.; Worek, W.M. *Solar Engineering of Thermal Processes*, 4th ed.; Wiley: New York, NY, USA, 2003; Volume 116.
11. Li, D.H.W.; Lou, S.W.; Lam, J.C. An Analysis of Global, Direct and Diffuse Solar Radiation. In *Energy Procedia*; Elsevier B.V.: Amsterdam, The Netherlands, 2015; Volume 75, pp. 388–393.
12. Gueymard, C. Critical analysis and performance assessment of clear sky solar irradiance models using theoretical and measured data. *Sol. Energy* **1993**, *51*, 385–397. [[CrossRef](#)]
13. Yadav, A.K.; Chandel, S.S. Solar radiation prediction using Artificial Neural Network techniques: A review. *Renew. Sustain. Energy Rev.* **2014**, *33*, 772–781. [[CrossRef](#)]
14. *ASHRAE Handbook, 1985 Fundamentals*; American Society of Heating Refrigerating and Air-Conditioning Engineers, Inc.: Atlanta, GA, USA, 2011.
15. Machler, M.A.; Iqbal, M. A modification of the ASHRAE clear sky irradiation model. *ASHRAE Trans.* **1967**, *91*, 106–115.
16. Parishwad, G.; Bhardwaj, R.K.; Nema, V.K. Estimation of hourly solar radiation for India. *Renew. Energy* **1997**, *12*, 303–313. [[CrossRef](#)]
17. Nijegorodov, N. Improved ashrae model to predict hourly and daily solar radiation components in Botswana, Namibia, and Zimbabwe. *WREC* **1996**, *9*, 1270–1273. [[CrossRef](#)]

18. Kumar, R.; Umanand, L. Estimation of global radiation using clearness index model for sizing photovoltaic system. *Renew. Energy* **2005**, *30*, 2221–2233. [[CrossRef](#)]
19. Ayodele, T.R.; Ogunjuyigbe, A.S.O. Prediction of monthly average global solar radiation based on statistical distribution of clearness index. *Energy* **2015**, *90*, 1733–1742. [[CrossRef](#)]
20. Chandrasekaran, J.; Kumar, S. Hourly diffuse fraction correlation at a tropical location. *Sol. Energy* **1994**, *53*, 505–510. [[CrossRef](#)]
21. Erbs, D.G.; Klein, S.A.; Duffie, J.A. Estimation of the diffuse radiation fraction for hourly, daily and monthly-average global radiation. *Sol. Energy* **1982**, *28*, 293–302. [[CrossRef](#)]
22. Hawlader, M.N.A. Diffuse, global and extra-terrestrial solar radiation for Singapore. *Int. J. Ambient Energy* **1984**, *5*, 31–38. [[CrossRef](#)]
23. Jacovides, C.P.; Tymvios, F.S.; Assimakopoulos, V.D.; Kaltsounides, N.A. Comparative study of various correlations in estimating hourly diffuse fraction of global solar radiation. *Renew. Energy* **2006**, *31*, 2492–2504. [[CrossRef](#)]
24. Karatasou, S.; Santamouris, M.; Geros, V. Analysis of experimental data on diffuse solar radiation in Athens, Greece, for building applications. *Int. J. Sustain. Energy* **2003**, *23*, 1–11. [[CrossRef](#)]
25. Lam, J.C.; Li, D.H.W. Correlation between global solar radiation and its direct and diffuse components. *Build. Environ.* **1996**, *31*, 527–535. [[CrossRef](#)]
26. Louche, A.; Poggi, P.; Simonnot, G.; Sanguinaires, R. Correlations for direct normal and global horizontal irradiation on a french mediterranean site. *Sol. Energy* **1991**, *46*, 261–266. [[CrossRef](#)]
27. De Miguel, A.; Bilbao, J.; Aguiar, R.; Kambezidis, H.; Negro, E. Diffuse solar irradiation model evaluation in the North Mediterranean Belt area. *Sol. Energy* **2001**, *70*, 143–153. [[CrossRef](#)]
28. Orgill, J.F.; Hollands, K.G.T. Correlation equation for hourly diffuse radiation on a horizontal surface. *Sol. Energy* **1977**, *19*, 357–359. [[CrossRef](#)]
29. Boland, J.; Scott, L.; Luther, M. Modelling the diffuse fraction of global solar radiation on a horizontal surface. *Environmetrics* **2001**, *12*, 103–116. [[CrossRef](#)]
30. Liu, B.Y.H.; Jordan, R.C. The interrelationship and characteristic distribution of direct, diffuse and total solar radiation. *Sol. Energy* **1960**, *4*, 1–19. [[CrossRef](#)]
31. Spencer, J.W. A comparison of methods for estimating hourly diffuse solar radiation from global solar radiation. *Sol. Energy* **1982**, *29*, 19–32. [[CrossRef](#)]
32. Oliveira, A.P.; Escobedo, J.F.; Machado, A.J.; Soares, J. Correlation models of diffuse solar-radiation applied to the city of São Paulo, Brazil. *Appl. Energy* **2002**, *71*, 59–73. [[CrossRef](#)]
33. Soares, J.; Oliveira, A.P.; Božnar, M.Z.; Mlakar, P.; Escobedo, J.F.; Machado, A.J. Modeling hourly diffuse solar-radiation in the city of São Paulo using a neural-network technique. *Appl. Energy* **2004**, *79*, 201–214. [[CrossRef](#)]
34. Radiation, G.; New, F.O.R. Correlation between hourly diffuse and. *Energy Convers. Manag.* **1984**, *24*, 265–267.
35. Al-Rawahi, N.Z.; Zurigat, Y.H.; Al-Azri, N.A. Prediction of hourly solar radiation on horizontal and inclined surfaces for Muscat/Oman. *J. Eng. Res.* **2011**, *8*, 19–31.
36. Bird, R.E.; Hulstrom, R.L. *A Simplified Clear Sky Model for Direct and Diffuse Insolation on Horizontal Surface*; Solar Energy Research Institute: Golden, CO, USA, 1981; p. 46.
37. Maxwell, E.L. METSTAT—The solar radiation model used in the production of the national solar radiation data base (NSRDB). *Sol. Energy* **1998**, *62*, 263–279. [[CrossRef](#)]
38. Yang, K.; Koike, T. A general model to estimate hourly and daily solar radiation for hydrological studies. *Water Resour. Res.* **2005**, *41*, 1–13. [[CrossRef](#)]
39. Gueymard, C.A. REST2: High-performance solar radiation model for cloudless-sky irradiance, illuminance, and photosynthetically active radiation—Validation with a benchmark dataset. *Sol. Energy* **2008**, *82*, 272–285. [[CrossRef](#)]
40. Ineichen, P. A broadband simplified version of the Solis clear sky model. *Sol. Energy* **2008**, *82*, 758–762. [[CrossRef](#)]
41. Engerer, N.A. Minute resolution estimates of the diffuse fraction of global irradiance for southeastern Australia. *Sol. Energy* **2015**, *116*, 215–237. [[CrossRef](#)]
42. Yao, W.; Li, Z.; Xiu, T.; Lu, Y.; Li, X. New decomposition models to estimate hourly global solar radiation from the daily value. *Sol. Energy* **2015**, *120*, 87–99. [[CrossRef](#)]

43. Gueymard, C. Mean daily averages of beam radiation received by tilted surfaces as affected by the atmosphere. *Sol. Energy* **1986**, *37*, 261–267. [[CrossRef](#)]
44. Kuo, C.-W.; Chang, W.-C.; Chang, K.-C. Modeling the hourly solar diffuse fraction in Taiwan. *Renew. Energy* **2014**, *66*, 56–61. [[CrossRef](#)]
45. Chendo, M.A.C.; Maduekwe, A.A.L. DATA BANK Hourly distributions of global and diffuse solar radiation in Lagos, Nigeria. *Renew. Energy* **1994**, *4*, 101–108. [[CrossRef](#)]
46. Chikh, M.; Mahrane, A.; Haddadi, M. Modeling the diffuse part of the global solar radiation in Algeria. *Energy Procedia* **2012**, *18*, 1068–1075. [[CrossRef](#)]
47. Dervishi, S.; Mahdavi, A. Comparison of models for the derivation of diffuse fraction of global irradiance data for Vienna, Austria. In Proceedings of the Building Simulation 2011—12th Conference of International Building Performance Simulation Association, Sydney, Australia, 14–16 November 2011; pp. 760–771.
48. Badescu, V. 3D isotropic approximation for solar diffuse irradiance on tilted surfaces. *Renew. Energy* **2002**, *26*, 221–233. [[CrossRef](#)]
49. Koronakis, P.S. On the choice of the angle of tilt for south facing solar collectors in the Athens basin area. *Sol. Energy* **1986**, *36*, 217–225. [[CrossRef](#)]
50. Liu, B.; Jordan, R. Daily insolation on surfaces tilted towards equator. *ASHRAE* **1961**, *10*, 53–59.
51. Tian, Y.Q.; Davies-Colley, R.J.; Gong, P.; Thorrold, B.W. Estimating solar radiation on slopes of arbitrary aspect. *Agric. For. Meteorol.* **2001**, *109*, 67–74. [[CrossRef](#)]
52. Bugler, J.W. The determination of hourly insolation on an inclined plane using a diffuse irradiance model based on hourly measured global horizontal insolation. *Sol. Energy* **1977**, *19*, 477–491. [[CrossRef](#)]
53. Temps, R.C.; Coulson, K.L. Solar radiation incident upon slopes of different orientations. *Sol. Energy* **1977**, *19*, 179–184. [[CrossRef](#)]
54. Hay, J.; Davies, J. Calculation of monthly mean solar radiation for horizontal and inclined surfaces. *Sol. Energy* **1980**, *23*, 301–307. [[CrossRef](#)]
55. Reindl, D.T. Evaluation of hourly tilted surface radiation models. *Sol. Energy* **1990**, *45*, 9–17. [[CrossRef](#)]
56. Klucher, T.M. Evaluation of models to predict insolation on tilted surfaces. *Sol. Energy* **1979**, *23*, 111–114. [[CrossRef](#)]
57. Arvid Skartveit, J.A.O. A model for the diffuse fraction of hourly global radiation. *Sol. Energy* **1987**, *38*, 271–274. [[CrossRef](#)]
58. Willmott, C.J. On the climatic optimization of the tilt and azimuth of flat-plate solar collectors. *Sol. Energy* **1982**, *28*, 205–216. [[CrossRef](#)]
59. Perez, R.; Stewart, R.; Seals, R.; Guertin, T. *The Development and Verification of the Perez Diffuse Radiation Model*; Sandia National Labs.: Albuquerque, NM, USA; State University of New York: Albany, NY, USA, 1988.
60. Perez, R.; Ineichen, P.; Seals, R.; Michalsky, J.; Stewart, R. Modeling daylight availability and irradiance components from direct and global irradiance. *Sol. Energy* **1990**, *44*, 271–289. [[CrossRef](#)]
61. Dal Pai, A.; Escobedo, J.F.; Dal Pai, E.; dos Santos, C.M. Estimation of Hourly, Daily and Monthly Mean Diffuse Radiation Based on MEO Shadowring Correction. *Energy Procedia* **2014**, *57*, 1150–1159. [[CrossRef](#)]
62. Khoo, Y.S.; Nobre, A.; Malhotra, R.; Yang, D.; Ruther, R.; Reindl, T.; Aberle, A.G. Optimal orientation and tilt angle for maximizing in-plane solar irradiation for PV applications in Singapore. *IEEE J. Photovolt.* **2014**, *4*, 647–653. [[CrossRef](#)]
63. Gulin, M.; Vasak, M.; Baotic, M. Estimation of the global solar irradiance on tilted surfaces. In Proceedings of the 17th International Conference on Electrical Drives and Power Electronics, Dubrovnik, Croatia, 2–4 October 2013; p. 6.
64. Souza, A.P.; Escobedo, J.F. Estimates of Hourly Diffuse Radiation on Tilted Surfaces in Southeast of Brazil. *Int. J. Renew. Energy Res.* **2013**, *3*, 207–221.
65. Frydrychowicz-Jastrzębska, G.; Bugała, A. Modeling the Distribution of Solar Radiation on a Two-Axis Tracking Plane for Photovoltaic Conversion. *Energies* **2015**, *8*, 1025–1041. [[CrossRef](#)]
66. Włodarczyk, D.; Nowak, H. Statistical analysis of solar radiation models onto inclined planes for climatic conditions of Lower Silesia in Poland. *Arch. Civ. Mech. Eng.* **2009**, *9*, 127–144. [[CrossRef](#)]
67. Elminir, H.K.; Ghitas, A.E.; El-Hussainy, F.; Hamid, R.; Beheary, M.M.; Abdel-Moneim, K.M. Optimum solar flat-plate collector slope: Case study for Helwan, Egypt. *Energy Convers. Manag.* **2006**, *47*, 624–637. [[CrossRef](#)]

68. Diez-Mediavilla, M.; de Miguel, A.; Bilbao, J. Measurement and comparison of diffuse solar irradiance models on inclined surfaces in Valladolid (Spain). *Energy Convers. Manag.* **2005**, *46*, 2075–2092. [[CrossRef](#)]
69. Mehleri, E.D.; Zervas, P.L.; Sarimveis, H.; Palyvos, J.A.; Markatos, N.C. A new neural network model for evaluating the performance of various hourly slope irradiation models: Implementation for the region of Athens. *Renew. Energy* **2010**, *35*, 1357–1362. [[CrossRef](#)]
70. Muneer, T. *Solar Radiation and Daylight Models for the Energy Efficient Design of Buildings*, 2nd ed.; Butterworth-Heinemann: London, UK, 2004.
71. Coffari, E. The sun and the celestial vault. In *Solar Energy Engineer*; Academic Press: New York, NY, USA, 1977.
72. Gueymard, C. An anisotropic solar irradiance model for tilted surfaces and its comparison with selected engineering algorithms. *Sol. Energy* **1987**, *38*, 367–386. [[CrossRef](#)]
73. Gueymard, C.A. Direct and indirect uncertainties in the prediction of tilted irradiance for solar engineering applications. *Sol. Energy* **2009**, *83*, 432–444. [[CrossRef](#)]
74. Shukla, K.N.; Rangnekar, S.; Sudhakar, K. Comparative study of isotropic and anisotropic sky models to estimate solar radiation incident on tilted surface: A case study for Bhopal, India. *Energy Rep.* **2015**, *1*, 96–103. [[CrossRef](#)]
75. Page, J. The estimation of monthly mean values of daily total short wave radiation on vertical and inclined surfaces from sunshine records 40S–40N. In *Proceedings of the United Nations Conference on New Sources of Energy: Solar Energy, Wind Power and Geothermal Energy*, Rome, Italy, 21–31 August 1967; pp. 378–390.
76. Tarhan, S.; Sari, A. Model selection for global and diffuse radiation over the Central Black Sea (CBS) region of Turkey. *Energy Convers. Manag.* **2005**, *46*, 605–613. [[CrossRef](#)]
77. Barbaro, S.; Cannata, G.; Coppolino, S.; Leone, C.; Sinagra, E. Diffuse solar radiation statistics for Italy. *Sol. Energy* **1981**, *26*, 429–435. [[CrossRef](#)]
78. Aras, H.; Balli, O.; Hepbasli, A. Estimating the horizontal diffuse solar radiation over the Central Anatolia Region of Turkey. *Energy Convers. Manag.* **2006**, *47*, 2240–2249. [[CrossRef](#)]
79. Liu, B.Y.H.; Jordan, R.C. A Rational Procedure for Predicting The Long-Term Average Performance of Flat-Plate Solar-Energy Collectors. *Sol. Energy* **1963**, *7*, 53–74. [[CrossRef](#)]
80. Farhan, S.F.; Tabbassum, K.; Talpur, S.; Alvi, B.M.; Liao, X.; Dong, L. Electrical Power and Energy Systems Evaluation of solar energy resources by establishing empirical models for diffuse solar radiation on tilted surface and analysis for optimum tilt angle for a prospective location in southern region of Sindh, Pakistan. *Int. J. Electr. Power Energy Syst.* **2015**, *64*, 1073–1080.
81. Lee, K.; Yoo, H.; Levermore, G.J. Quality control and estimation hourly solar irradiation on inclined surfaces in South Korea. *Renew. Energy* **2013**, *57*, 190–199. [[CrossRef](#)]
82. Noorian, A.M.; Moradi, I.; Kamali, G.A. Evaluation of 12 models to estimate hourly diffuse irradiation on inclined surfaces. *Renew. Energy* **2008**, *33*, 1406–1412. [[CrossRef](#)]
83. Notton, G.; Poggi, P.; Cristofari, C. Predicting hourly solar irradiances on inclined surfaces based on the horizontal measurements: Performances of the association of well-known mathematical models. *Energy Convers. Manag.* **2006**, *47*, 1816–1829. [[CrossRef](#)]
84. Padovan, A.; Col, D. Del Measurement and modeling of solar irradiance components on horizontal and tilted planes. *Sol. Energy* **2010**, *84*, 2068–2084. [[CrossRef](#)]
85. The Chartered Institution of Building Services Engineers. Available online: <http://www.cibse.org/getmedia/4f58cd6d-9335--49ae-bade-74106690e3c9/Guide-A-presentation.pdf.aspx> (accessed on 19 September 2016).
86. Klein, S.A. Calculation of monthly average insolation on tilted surfaces. *Sol. Energy* **1977**, *19*, 325–329. [[CrossRef](#)]
87. Khatib, T. A Review of Designing, Installing and Evaluating Standalone Photovoltaic Power Systems. *J. Appl. Sci.* **2010**, *10*, 1212–1228. [[CrossRef](#)]
88. Sinha, S.; Chandel, S.S. Analysis of fixed tilt and sun tracking photovoltaic-micro wind based hybrid power systems. *Energy Convers. Manag.* **2016**, *115*, 265–275. [[CrossRef](#)]
89. Khorasanizadeh, H.; Mohammadi, K.; Mostafaiepour, A. Establishing a diffuse solar radiation model for determining the optimum tilt angle of solar surfaces in Tabass, Iran. *Energy Convers. Manag.* **2014**, *78*, 805–814. [[CrossRef](#)]
90. Jafarkazemi, F.; Saadabadi, S.A. Optimum tilt angle and orientation of solar surfaces in Abu Dhabi, UAE. *Renew. Energy* **2013**, *56*, 44–49. [[CrossRef](#)]

91. Klein, S.A.; Theilacker, J.C. Algorithm for Calculating Monthly-Average Radiation on Inclined Surfaces. *J. Sol. Energy Eng. Trans. ASME* **1981**, *103*, 29–33. [[CrossRef](#)]
92. Bakirci, K. General models for optimum tilt angles of solar panels: Turkey case study. *Renew. Sustain. Energy Rev.* **2012**, *16*, 6149–6159. [[CrossRef](#)]
93. Ertekin, C.; Evrendilek, F.; Kulcu, R. Modeling spatio-temporal dynamics of optimum tilt angles for solar collectors in Turkey. *Sensors* **2008**, *8*, 2913–2931. [[CrossRef](#)] [[PubMed](#)]
94. Zhao, Q.; Wang, P.; Goel, L. Optimal PV panel tilt angle based on solar radiation prediction. In Proceedings of the 2010 IEEE 11th International Conference on Probabilistic Methods Applied to Power Systems (PMAPS), Singapore, 14–17 June 2010; pp. 425–430.
95. Liu, L.-M.; Hudak, G.B.; Box, G.E.P.; Muller, M.E.; Tiao, G.C. *Forecasting and Time Series Analysis Using the SCA Statistical System*; Scientific Computing Associates: DeKalb, IL, USA, 1992.
96. Maru, N.; Vajpai, J. Model based Optimization of Tilt angle for Solar PV Panels in Jodhpur. In Proceedings of the National Conference on Intelligent Systems (NCIS 2014), Jodhpur, India, 22–23 December 2014; pp. 32–39.
97. Kazem, H.A.; Khatib, T.; Alwaeli, A.A.K. Optimization of photovoltaic modules tilt angle for Oman. In Proceedings of the 2013 IEEE 7th International Power Engineering and Optimization Conference, PEOCO 2013, Langkawi, Malaysia, 3–4 June 2013; pp. 703–707.
98. Ismail, M.S.; Moghavvemi, M.; Mahlia, T.M.I. Analysis and evaluation of various aspects of solar radiation in the Palestinian territories. *Energy Convers. Manag.* **2013**, *73*, 57–68. [[CrossRef](#)]
99. Jain, P.C. Estimation of monthly average hourly global and diffuse irradiation. *Sol. Wind Technol.* **1988**, *5*, 7–14. [[CrossRef](#)]
100. Despotovic, M.; Nedic, V. Comparison of optimum tilt angles of solar collectors determined at yearly, seasonal and monthly levels. *Energy Convers. Manag.* **2015**, *97*, 121–131. [[CrossRef](#)]



© 2017 by the authors; licensee MDPI, Basel, Switzerland. This article is an open access article distributed under the terms and conditions of the Creative Commons Attribution (CC BY) license (<http://creativecommons.org/licenses/by/4.0/>).